Pictorial Essay

Anatomy of the Jaw Revisited with a Dental CT Software Program

James J. Abrahams

Summary: The jaw has traditionally been evaluated by dentists and oral surgeons using conventional panoramic and intraoral films. Recently, CT software programs specifically developed to evaluate dental implant patients have provided radiologists with a new look at the mandible and maxilla. The anatomy seen on these reformatted panoramic and cross-sectional images is complex, and our objective is to define it. By the use of standard anatomic drawings, mandibular and maxillary anatomy was identified on human skulls and then on the axial, cross-sectional, and panoramic DentaScan images of these skulls. With this anatomic description, the DentaScans from several representative patients were then used to portray mandibular and maxillary anatomy in a pictorial fashion.

Index terms: Mandible; Maxilla; Computed tomography, software

In the past few years, the need for involvement by the radiologist in mandibular and maxillary imaging has increased because of the development of dental implants. These are titanium cylinders that are surgically implanted into the jaw to permit the fixation of permanent dentures (1) (Fig. 1). The success of this procedure requires the oral surgeon to know the precise location of the mandibular canal (neurovascular bundle) and the maxillary sinuses and the height, width, and contour of the alveolar process. Routine panoramic radiographs are not optimal for this type of evaluation. They are unable to determine the width of the mandible and have up to 25% distortion. Axial computed tomography (CT) is also limited because much of the anatomy runs parallel to the plane of the scan. Direct coronal CT imaging has been unsuccessful because of streak artifact created from dental restorations and the degree of hyperextension required of the patient.

To improve imaging of the mandible and maxilla, a dental CT reformatting program was developed that displays multiple axial, panoramic, and cross-sectional images of the jaw (Fig. 2) (2–4). This program is now being used extensively for evaluating patients with dental implants; its use for evaluating cysts (5), tumors (6), and fractures (9) is evolving. The purpose of this study is to identify anatomic landmarks on reformatted mandibular and maxillary CT images and to relate them to neurovascular and muscular structures.

Material and Methods

Standard anatomic drawings were used to identify mandibular and maxillary anatomy on dried human skulls. This anatomy was then identified on the axial, cross-sectional, and panoramic DentaScan (GE Medical Systems, Milwaukee, WI) images of these skulls. By the use of this anatomic description, the anatomy of the jaw was finally portrayed in a pictorial fashion on the DentaScans of several representative patients. DentaScans from patients provide soft-tissue density and more usable information than the dried specimens.

All scans were performed on a GE 9800 CT scanner. Axial sections were acquired parallel to the alveolar process by the use of a bone algorithm, dynamic mode, 15-cm field of view, 512 × 512 matrix, and section thickness of 1.5 mm with a 0.5-mm overlap in the mandible and no overlap in the maxilla. Data were then reformatted with DentaScan software. A curved line is first superimposed on one of the axial images of the jaw. The technologist does this by placing several dots along the curve of the jaw using the cursor on the console. The program then connects the dots to produce the curved line (Fig. 2A). The panoramic views (Fig. 2C) are then reformatted parallel to this line. The cross-sectional views (Fig. 2D through F) (which are unique to these programs) are reformatted along multiple numbered lines, which the program automatically draws perpendicular to this curve. Figure 1 illustrates the plane and orientation of the cross-sectional image. The number in the lower right of each cross-sectional image (Fig. 2D through F) corresponds to the number of the perpendicular line. Cross-sectional image 1 is therefore through the distal right mandible, image 28 is through the midline, and image 53 (not shown) is through the distal left mandible. The buccal (BCL) and lingual (LNG) surfaces are

Received May 18, 1992; revision requested July 13; final revision received September 9 and accepted September 30.

Address reprint requests to James J. Abrahams, MD, Yale University School of Medicine, Department of Diagnostic Imaging, 333 Cedar Street, New Haven, CT 06510.

AJNR 14:979–990, Jul/Aug 1993 0195-6108/93/1404–0979

labeled on the second image from the left of each screen save. The maxilla is reformatted in a similar fashion. The axial, panoramic, and cross-sectional images are cross-referenced through a series of tick marks that run along the bottom and side of the images. For example, the mental foramen, which is seen on the 14th axial image adjacent to perpendicular line number 20 (Fig. 2A), is also identified on cross-sectional image number 20 (Fig. 2E), adjacent to the 14th tick mark from the bottom.

Mandible

The anatomy of the lingual, buccal, and superior surfaces of the mandible is identified and labeled on the anatomic specimen in Fig. 3A and B, 3C, and 3D, respectively. This anatomy is then identified on the cross-sectional, axial, and panoramic DentaScan images in Figures 2 and 4. Comparison with neurovascular and muscular anatomy is depicted in Figures 5 and 6.

Anatomic Specimen

Lingual surface right mandible

The neurovascular bundle (mandibular nerve and artery) enters the mandibular foramen (*MF* in Fig. 3A) on the lingual aspect, traverses the mandible in the inferior alveolar canal, and exits on the buccal surface through the mental foramen (*M* in Figs. 3C and 5A). Internally, small nutrient canals extend from the inferior alveolar canal toward the teeth (Fig. 5A). The mylohyoid nerve (Fig. 5B) splits from the mandibular nerve before entering the mandibular foramen and travels on the surface of the mandible in the mylohyoid groove (*Mg* in Fig. 3A). This nerve innervates the mylohyoid muscle (Fig. 6A, C, and D), which inserts on the mylohyoid line (*Ml* in Fig. 3A). The mylohyoid line is an important landmark, because it separates the oral cavity from the suprahyoid portion of the neck. Inferior to the mylohyoid line, the submandibular gland (Fig. 6A) is located in the submandibular fossa (*S* in Fig. 3A). Superior to the line, the sublingual fossa (*Sl* in Fig. 3A) houses the sublingual gland (Fig. 6A).

The genial tubercle (*Gt* in Fig. 3A and B) is situated in the midline and is typically composed of four bony outgrowths. The right and left genioglossus muscles insert on the two superior spines; the right and left geniohyoid muscles insert on the two inferior spines (Fig. 6C and D). The lingual foramen (*Lf* in Fig. 3B) lies just inferior to the genial tubercle and provides an opening through which the lingual and incisive arteries anastomose (Fig. 6A). The incisive artery is a small branch of the mandibular artery, which, instead of exiting the mental foramen, travels within the mandible toward the midline. Inferior and to either side of the genial tubercle are the digastric fossae (*D* in Fig. 3A and B) for the insertions of the anterior bellies of the digastric muscles (Fig. 6A). The temporalis muscle (Fig. 6B and C) inserts on the coronoid process (Cp in Fig. 3B), and the lateral pterygoid (Fig. 6B and D) inserts on the anterior lingual aspect of the condyle (Cd in Fig. 3A). The medial pterygoid (Fig. 6B and D) inserts on the inferior aspect of the mandible near the junction of the body and the ramus (*Mp* in Fig. 3A).

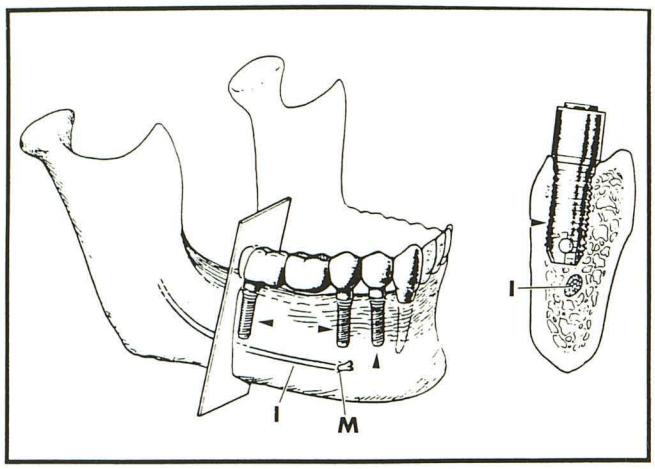

Fig. 1. View of the mandible illustrating the plane and orientation of the cross-sectional DentaScan image. The height and width of the alveolar process and the location of the mandibular canal can be determined on the cross-sectional image. Three dental implants are seen (*arrowheads*) supporting a four-tooth prosthesis. *I* indicates inferior alveolar canal; *M*, mental foramen.

Buccal surface right mandible

The coronoid process (Cp in Fig. 3C) merges with the body of the mandible to form the oblique line (*O* in Fig. 3C). Between the oblique line and the more medially (lingually) situated alveolar process (*A* in Fig. 3C) lies the insertion of the buccinator muscle (*B* in Fig. 3C and Fig. 6B and D). The deep and superficial portions of the masseter muscle (Fig. 6B and D) insert on the buccal surface of the ramus (*Mm* in Fig. 3C). Anteriorly, the mental foramen (*M* in Fig. 3C) exits inferior to the first and second bicuspids.

Superior surface left mandible

The most superior portion of the mandibular body is formed by the alveolar process, which houses the teeth. Posteriorly, it assumes a medial (lingual) position in relation to the mandibular body (Fig. 3D), because the curve of the alveolar process is more acute than that of the rest of the mandible. This is reflected in the cross-sectional DentaScan images (Fig. 2D, image 10). Posterior to the teeth, the alveolar process forms the retromolar triangle (*Rt* in Fig. 3D) and then becomes the temporal crest (*T* in Fig. 3D) as it merges with the lingual aspect of the ramus. The retromolar triangle, a bony structure, is to be distinguished from the soft-tissue retromolar trigone. Buccal to this, the anterior portion of the coronoid process (*Cp* in Fig. 3D) merges with the body of the mandible to form the oblique line (O in Fig. 3D). The retromolar fossa (*Rf* in Fig. 3D) is situated between the oblique line and the temporal crest. The lateral

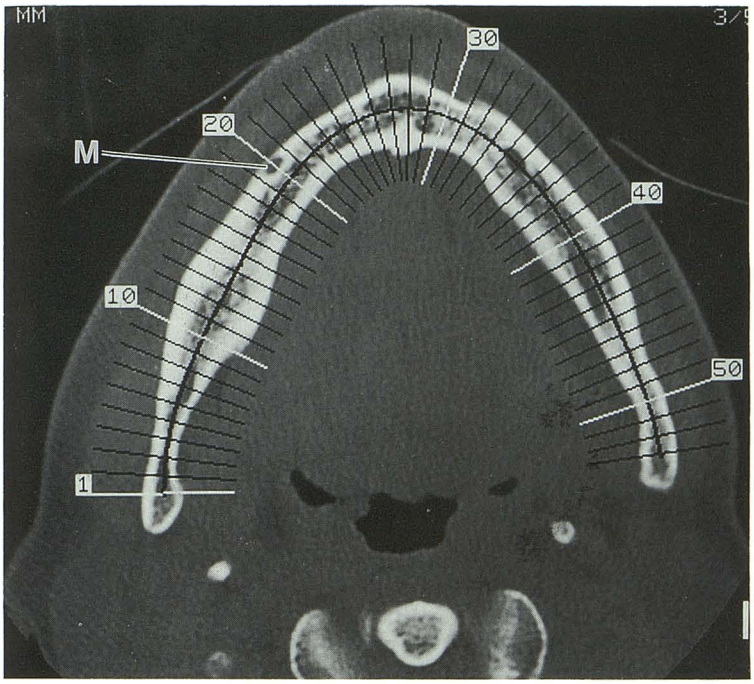

A

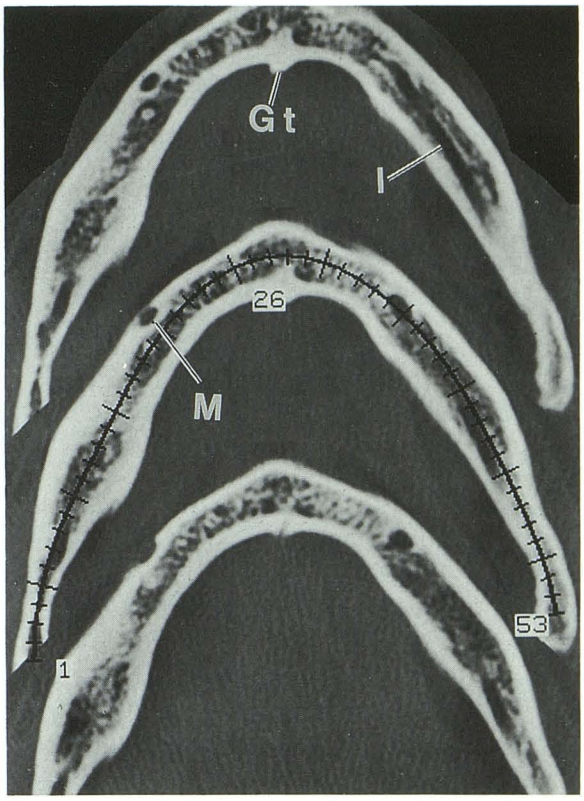

B

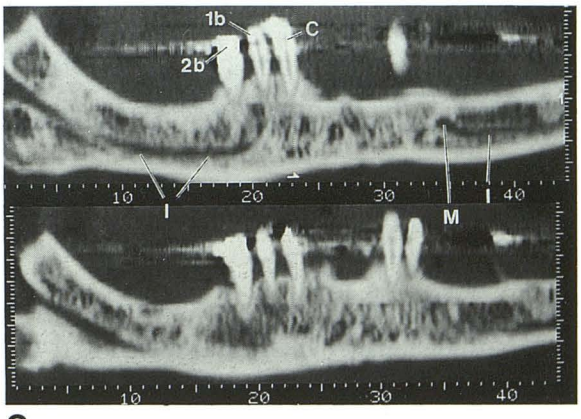

C

Fig. 2. DentaScan of mandible.

A, Axial view. The panoramic images seen in (*C*) are reformatted parallel to the curved line superimposed on this axial image. The numbered cross-sectional images in (*D* through *F*) are reformatted along the numbered lines drawn perpendicular to this curve. Cross-sectional image 1 is through the distal right mandible, image 27 is through the midline, and image 53 (not shown) is through the distal left mandible. *M* indicates mental foramen.

B, Axial images illustrating the inferior alveolar canal (*I*), the mental foramen (*M*), and the genial tubercle (*Gt*).

C, Panoramic views. *I* indicates inferior alveolar canal; *M*, mental foramen; *2B*, second bicuspid; *1B*, first bicuspid; and *C*, cuspid.

pterygoid muscle (Fig. 6B and D) inserts on the anterior lingual aspect of the condyle (*Lp* in Fig. 3D).

DentaScan Images: Cross-sectional View

Lingual Surface

The more distal cross-sectional images through the junction of the right ramus and body (images 1 through 5 in Fig. 2D) clearly demonstrate the mandibular foramen (*Mf*), the lingula (*L*), and the mylohyoid groove (*Mg*). Moving anteriorly (images 9 through 11 in Fig. 2D and E), the mylohyoid line (*Ml*), the submandibular fossa (*S*), and the sublingual fossa (*Sl*) are identified. Toward the midline (images 28 and 29 in Fig. 2F), the genial tubercle (*Gt*) and digastric fossa (*D*) can be seen. The superior (*Gt-g*) and inferior (*Gt-h*) processes of the genial tubercle, where the genioglossus and geniohyoid muscles insert, are better visualized in Figure 4C. Figure 4C also demonstrated the lingual foramen (*Lf*) just below the genial tubercle.

Buccal Surface

Posteriorly (images 4 through 7 in Fig. 2D), the coronoid process (*Cp*) merges with the body of the mandible to form the oblique line (*O*). Anteriorly (image 20 in Fig. 2E), the mental foramen (*M*) can be seen in cross-section. Note how clearly one can follow the course of the neurovascular bundle as it enters the mandibular foramen on the lingual

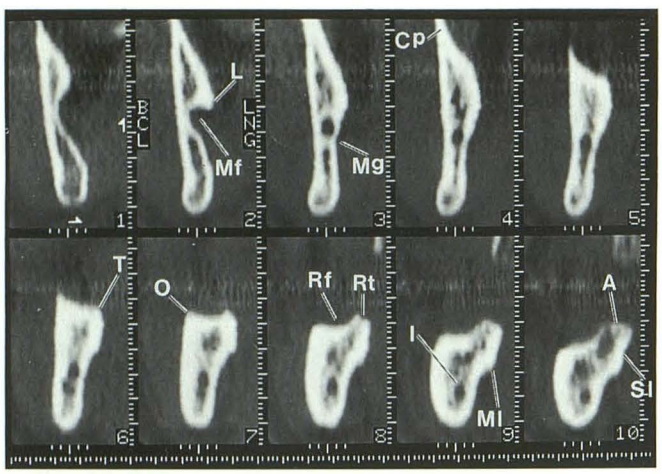

D

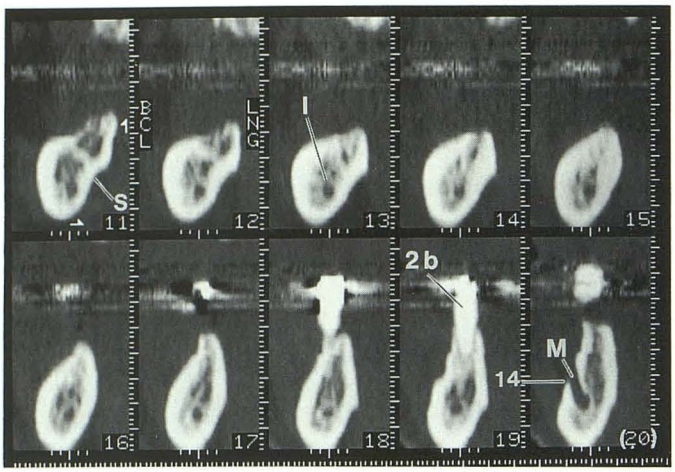

E

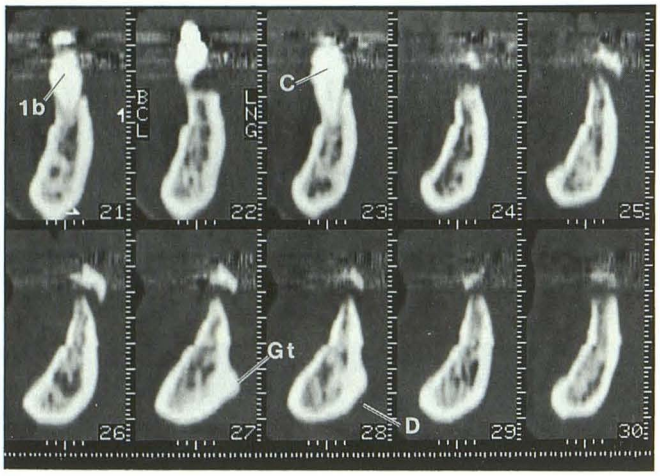

F

Fig. 2. Continued.

D through *F*, Cross-sectional views. Images 1 through 10 (*D*) are through the posterior right mandible (see perpendicular lines 1 through 10 in *A*). Images 11 through 20 (*E*) are more anterior. Images 21 through 30 (*F*) extend to the midline. The images of the left half of the mandible are not shown. Note how well mandibular anatomy is seen on the cross-sectional view. *14* marks the 14th tick mark, which corresponds to axial image 14 (see Materials and Methods for detail). *A* indicates alveolar process; *C*, cuspid; *Cp*, coronoid process; *D*, digastric fossa; *Gt*, genial tubercle; *I*, inferior alveolar canal; *L*, lingula; *M*, mental foramen; *Mf*, mandibular foramen; *Mg*, mylohyoid groove; *Ml*, mylohyoid line; *O*, oblique line; *Rf*, retromolar fossa; *Rt*, retromolar triangle; *S*, submandibular fossa; *Sl*, sublingual fossa; *T*, temporal crest; *1b*, first bicuspid; and *2b*, second bicuspid.

surface, travels through the inferior alveolar canal (*I*), and exits the mental foramen on the buccal surface.

Superior Surface

The inferior portion of the coronoid process (*Cp*) is seen extending off the images in Fig. 2D. As one moves from posterior to anterior (images 6 through 10 in Fig. 2D), the temporal crest (*T*) merges with the retromolar triangle (*Rt*) which ends in the alveolar process (*A*). The posterior teeth, which normally sit in the alveolar process, are absent in this partially edentulous mandible. Note how the alveolar process (*A*) assumes a lingual position in the posterior mandible (compare image 10 with image 19). The retromolar fossa (*Rf* in Fig. 2D) is identified between the oblique line and the temporal crest.

Internal Anatomy

Internally, the inferior alveolar canal (*I*) extends from the mandibular foramen to the mental foramen (*M*). The smaller canal for the incisive artery (*Ia*) is an extension of the inferior alveolar canal, which runs from the mental foramen (*M*) toward the midline (Fig. 4A and B). On the cross-sectional images, this can cause confusion, because it gives the appearance that the inferior alveolar canal extends anterior (mesial) to the mental foramen. To avoid confusion, one simply needs to remember that the canal on cross-sectional images distal to the mental foramen is the inferior alveolar canal; that mesial to it is the canal for the incisive artery. It has been my experience that implants placed mesial to the mental foramen (in the region of the canal for the incisive artery) do not cause sequelae like those typically experienced from injury to the inferior alveolar canal.

Axial View

The genial tubercle (*Gt*), mental foramen (*M*), and inferior alveolar canal (*I*) are identified in Figure 2A and B.

Panoramic View

The course of the inferior alveolar canal (*I* in Figs. 2C and 4A) and its exit point, the mental foramen (*M*), are clearly identified on the panoramic images. The canal for the incisive artery (*Ia*) travels from the mental foramen (*M*) toward the midline (Fig. 4A), and nutrient canals (*N*) extend from the inferior alveolar canal (*I*) toward the teeth.

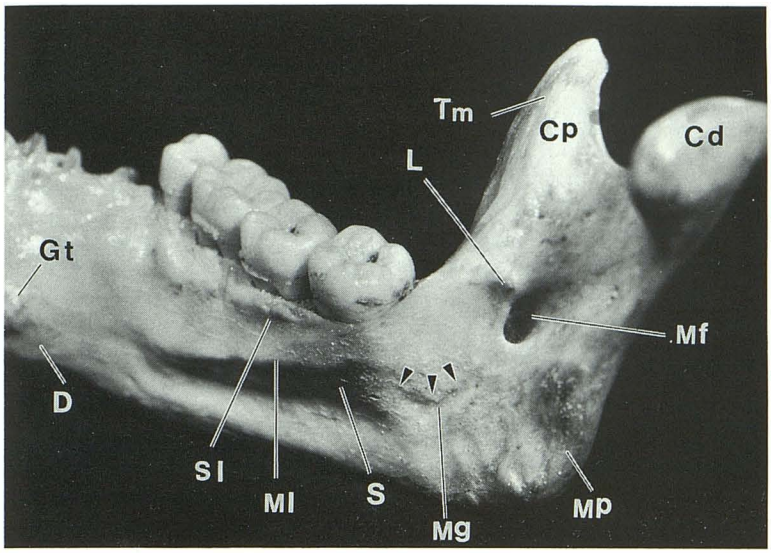

A

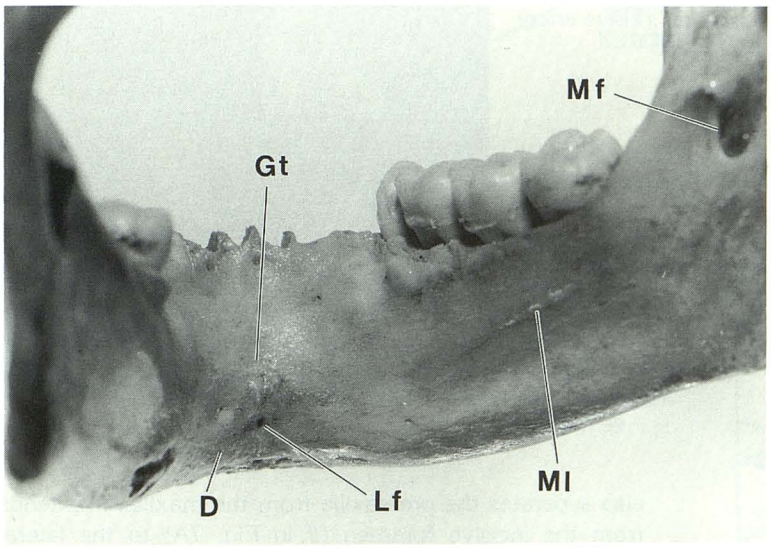

B

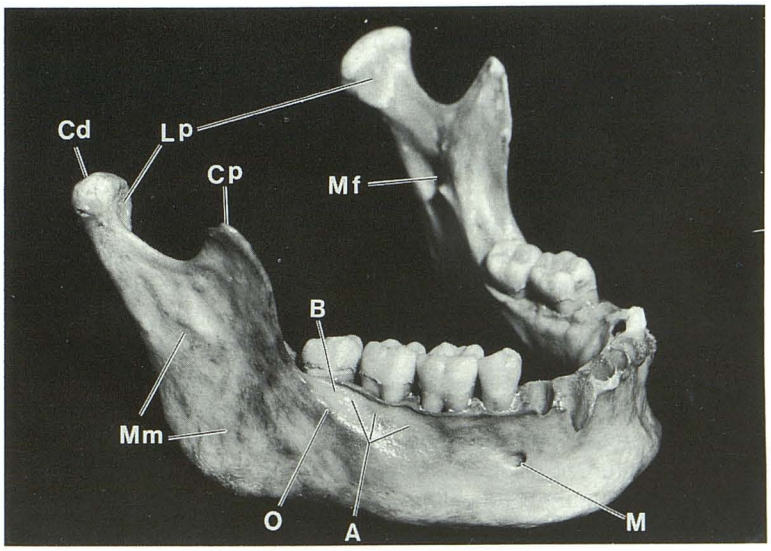

C

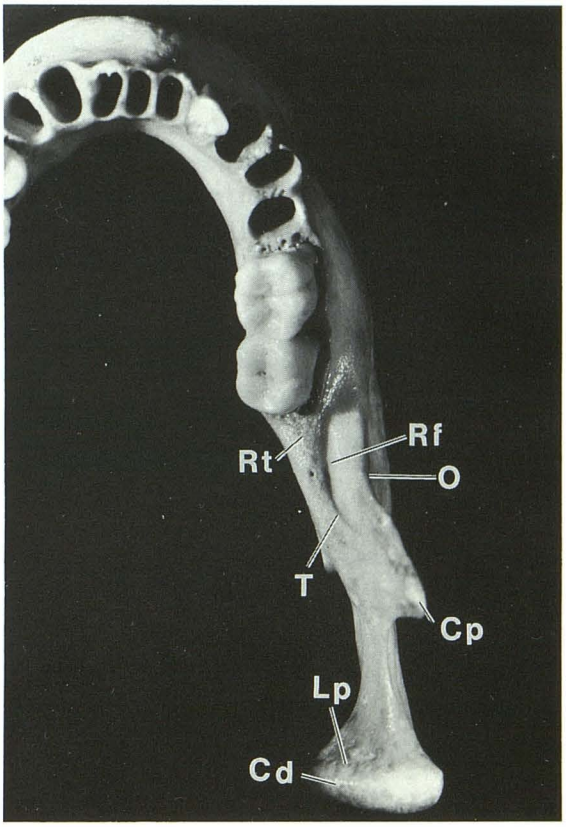

D

Fig. 3. Anatomic specimen demonstrating the lingual (*A* and *B*), buccal (*C*), and superior (*D*) aspect of the mandible. *A* indicates alveolar process; *B*, buccinator muscle insertion; *Cd*, condyle; *Cp*, coronoid process; *D*, digastric fossa; *Gt*, genial tubercle; *L*, lingula; *Lf*, lingual foramen; *Lp*, lateral pterygoid muscle insertion; *M*, mental foramen; *Mf*, mandibular foramen; *Mg*, mylohyoid groove; *Ml*, mylohyoid line; *Mm*, massetter muscle insertion; *Mp*, medial pterygoid insertion; *O*, oblique line; *Rf*, retromolar fossa; *Rt*, retromolar triangle; *S*, submandibular fossa; *Sl*, sublingual fossa; *T*, temporal crest; and *Tm*, temporalis muscle insertion.

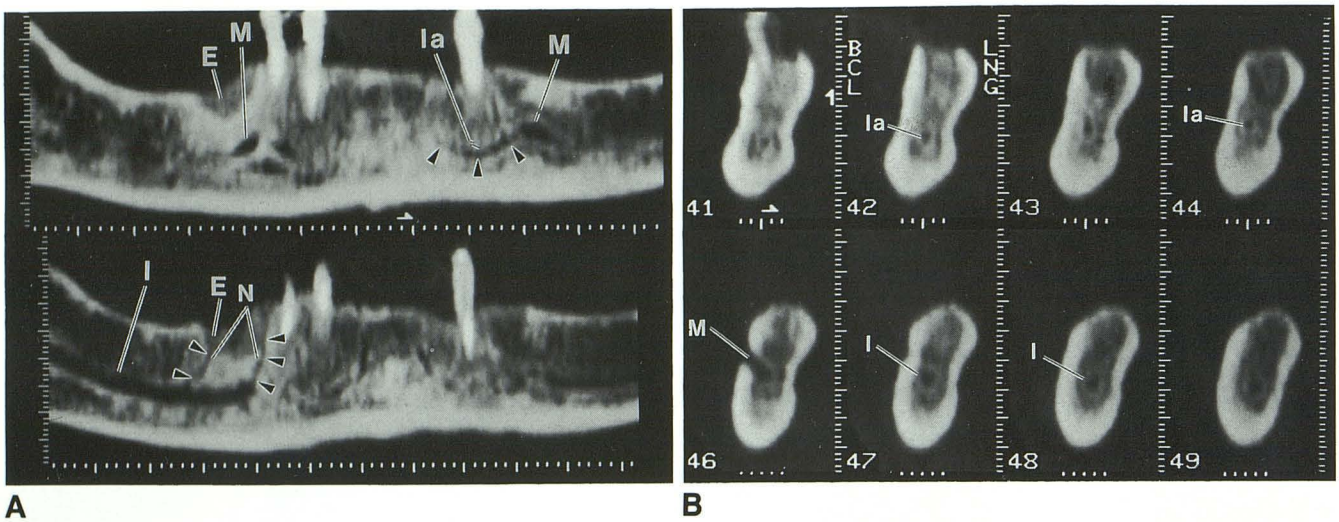

Fig. 4. Panoramic (*A*) and cross-sectional (*B* and *C*) DentaScan images demonstrating the incisive artery canal, the nutrient canals, and the lingual foramen. *E* indicates extraction socket; *Gt-g*, genial tubercle (genioglossus insertion); *Gt-h*, genial tubercle (geniohyoid insertion); *I*, inferior alveolar canal; *Ia*, incisive artery canal; *Lf*, lingual foramen; *M*, mental foramen; and *N*, nutrient canals.

Maxilla

The anatomy of the inferior, lateral, and frontal surfaces of the maxilla is identified and labeled on the anatomic specimen in Figure 7A, B, and C, respectively. This anatomy is then identified on the axial, panoramic, and cross-sectional DentaScan images in Figures 8 and 9. Correlation with the neurovascular anatomy is depicted in Figure 5B and C.

Anatomic Specimen

Inferior view

The hard palate is complex, being composed of several bones. The palatine process of the maxillary bone (*Mb* in Fig. 7A) is separated from the horizontal plate of the palatine bone (*Pb* in Fig. 7A) by the transverse suture (*Ts* in Fig. 7A). Posterior to the palatine bone, the pterygoid process (*Pt* in Fig. 7A) of the sphenoid bone is identified. A vertically oriented median palatine suture (*Mp* in Fig. 7A) then divides the bones of the palate into right and left halves. In younger patients, a horizontally oriented suture also separates the premaxilla from the maxilla. It extends from the incisive foramen (*If* in Fig. 7A) to the lateral incisor/cuspid region (*arrow* in Fig. 7A).

The teeth are housed in the alveolar process (*A* in Fig. 7A), an inferior extension of the hard palate, which assumes a curved configuration. Cephalad to it, one encounters the maxillary sinuses and nasal fossae. Posterior to the maxillary sinus and between it and the pterygoid process (*Pt* in Fig. 7A and B) lies the pterygopalatine fossa (*Tp* in Fig. 7B).

The second division of the trigeminal nerve enters the pterygopalatine fossa after exiting the skull base through the foramen rotundum (Fig. 5B). One of its branches, the pterygopalatine nerve, continues inferiorally through the pterygopalatine canal to exit the greater (*G* in Fig. 7A) and lesser (*L* in Fig. 7A) palatine foramina as the greater and lesser palatine nerves. A white probe, representing the greater palatine nerve, is seen exiting the greater palatine foramen (Fig. 7A). This nerve forms a groove (*Gg* in Fig. 7A) in the hard palate as it travels anteriomedially to supply sensory fibers to the posterior two thirds of the hard palate and teeth. The other end of the white probe (Fig. 7B)

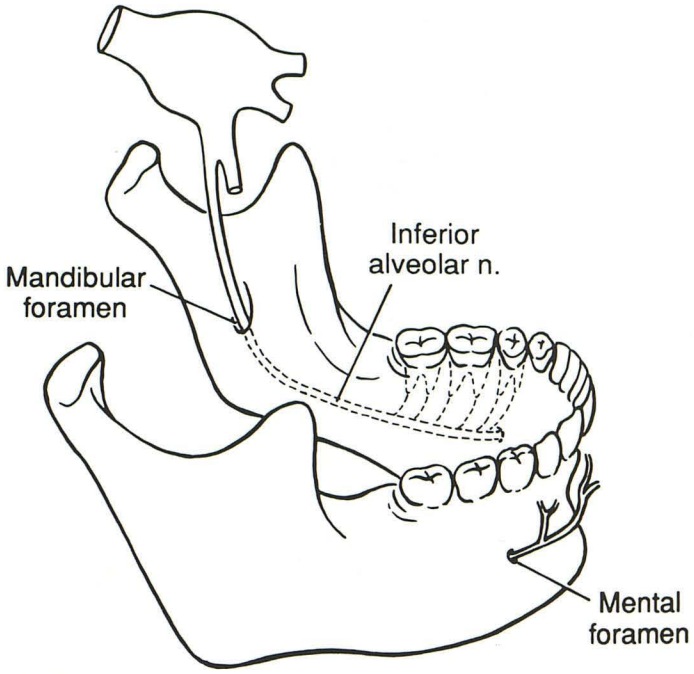

A

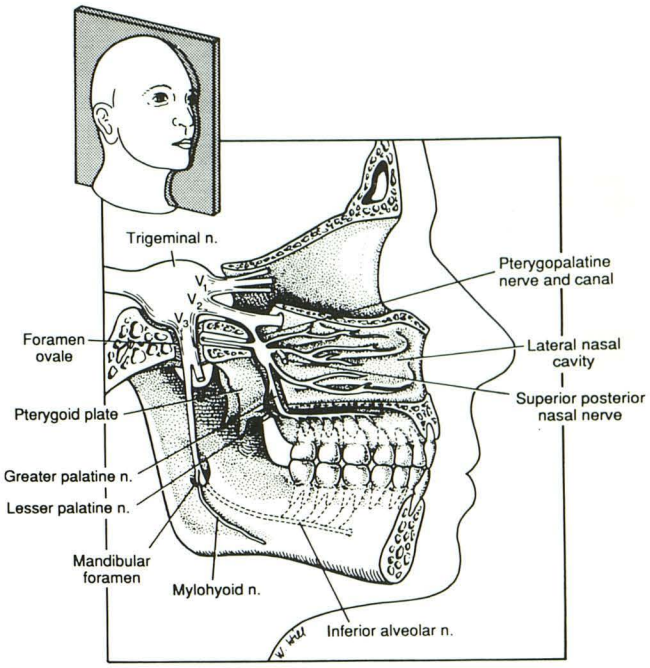

B

Fig. 5. Neurovascular structures.

A, View of the mandible illustrating the mandibular foramen, the mental foramen, and the nutrient canals, which extend from the inferior alveolar canal toward the teeth. *n* indicates nerve.

B, Parasagittal view through the trigeminal nerve and the lateral nasal cavity. Note how the myelohyoid nerve travels on the lingual surface of the mandible rather than entering the mandibular foramen. The greater palatine nerve arises from the pterygopalatine nerve, a branch of V2.

C, Midsagittal view through the incisive foramen and the nasal septum. Note how the nasopalatine nerve, a branch of the superior-posterior nasal nerve, travels along the nasal septum and through the incisive foramen.

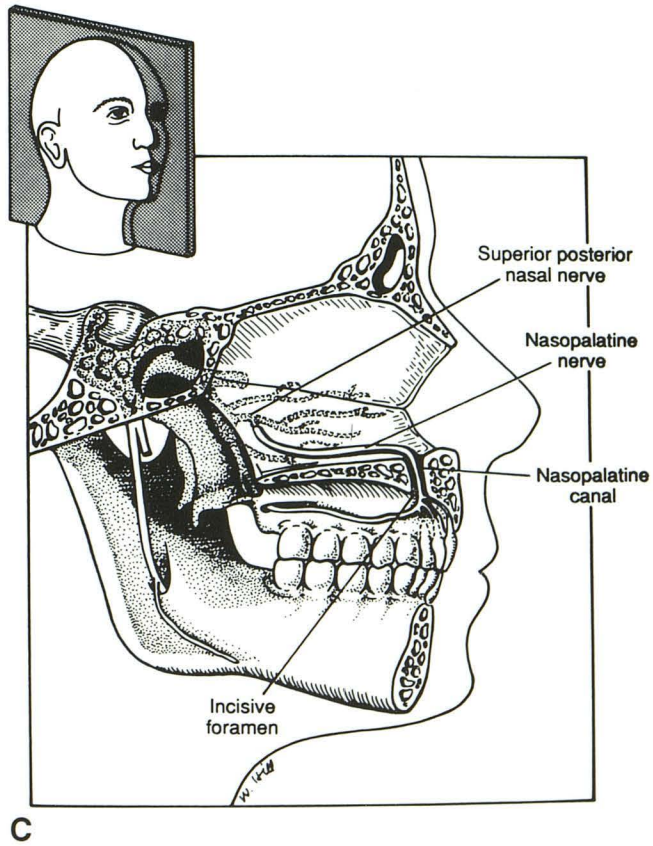

C

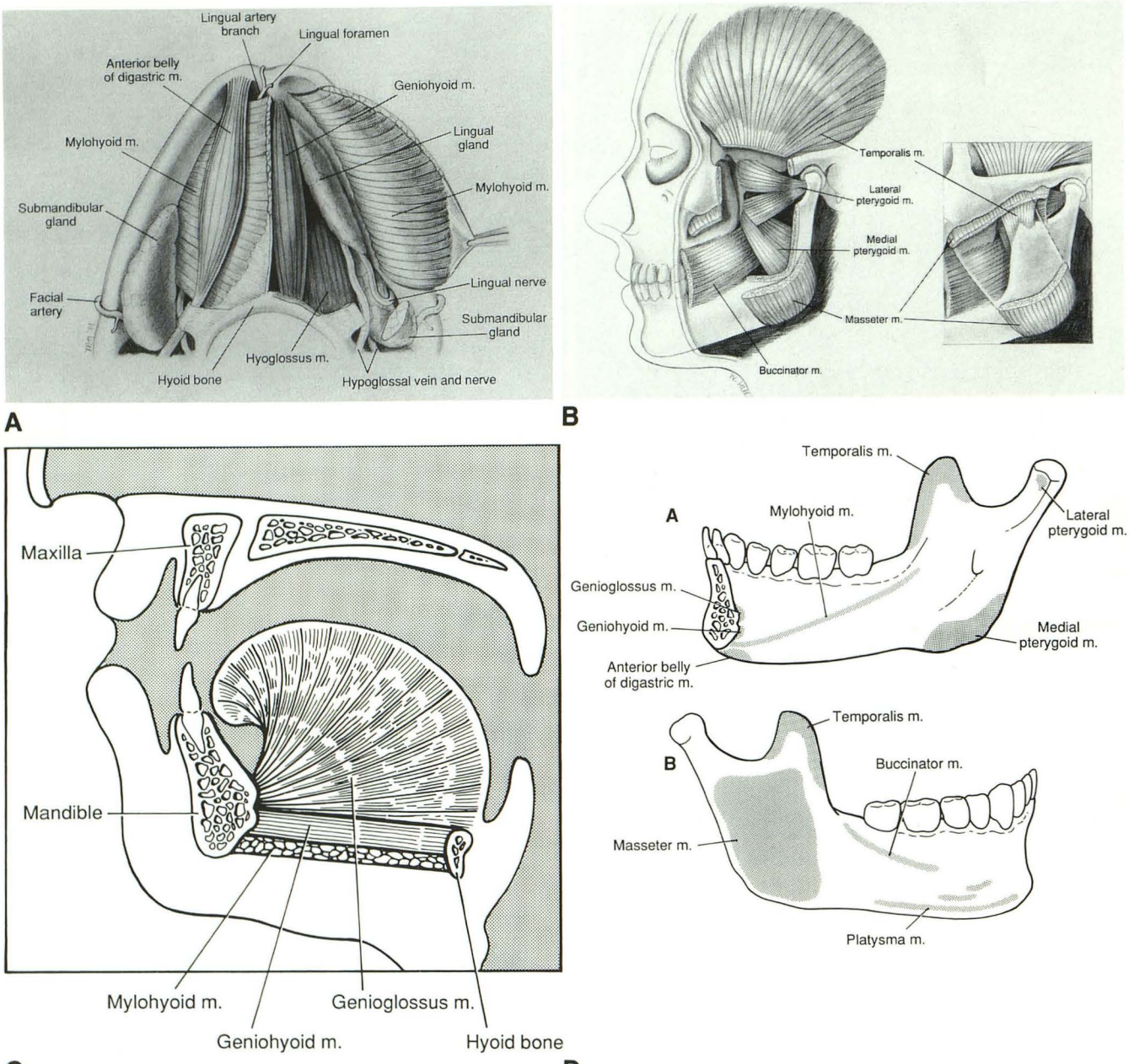

Fig. 6. Muscles and insertions.
A, Mandible viewed from below. *m* indicates muscle.
B, Lateral view with zygomatic arch and coronoid process removed.
C, Midline sagittal view through the genial tubercle.
D, Muscle insertions. Lingual surface (*A*). Buccal surface (*B*).

represents the pterygopalatine nerve and can be traced back into the pterygopalatine fossa (*Tp* in Fig. 7B).

The pterygopalatine nerve also gives rise to the superior posterior nasal nerve, which enters the posterior nasal cavity through the sphenopalatine foramen (Fig. 5C). After entering the nasal cavity, it gives off a medial branch, the nasopalatine nerve, which travels anterioinferiorly along the nasal septum to enter the nasopalatine canal (Figs. 5C and 7C). From here, it supplies sensory fibers to the central teeth (along with the anterior superior alveolar nerves, branches of the infraorbital nerve) and to the anterior hard palate; it then anastomoses with the terminal portion of the greater palatine nerve. The black probe in Figure 7A represents the course of the nasopalatine nerve. One end exits the incisive foramen (*If* in Fig. 7A), and the other travels through the nasopalatine canal (*Np* in Fig. 7C) and along the nasal septum (*Ns* in Fig. 7C) to merge with the superior posterior nasal nerve. There are two nasopalatine canals, a right and a left, each situated in the anterioinferior nasal fossa on either side of the nasal septum (*Ns* in Fig.

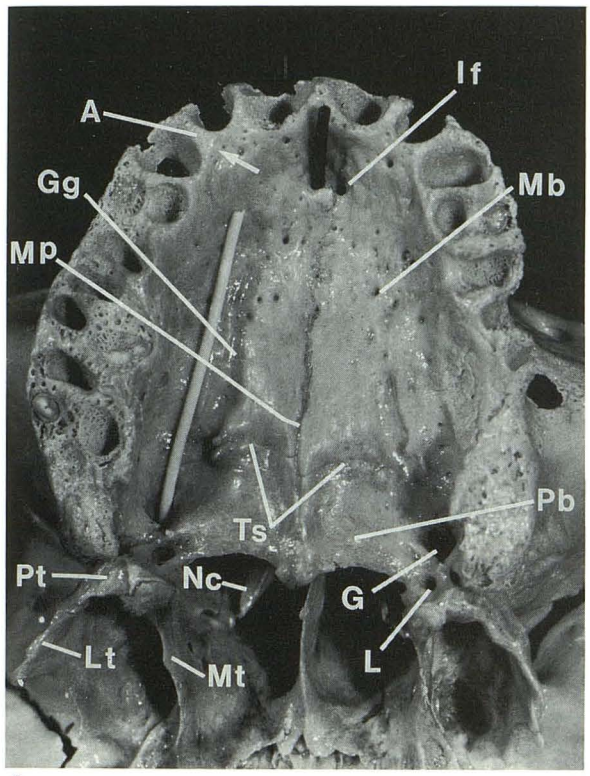

A

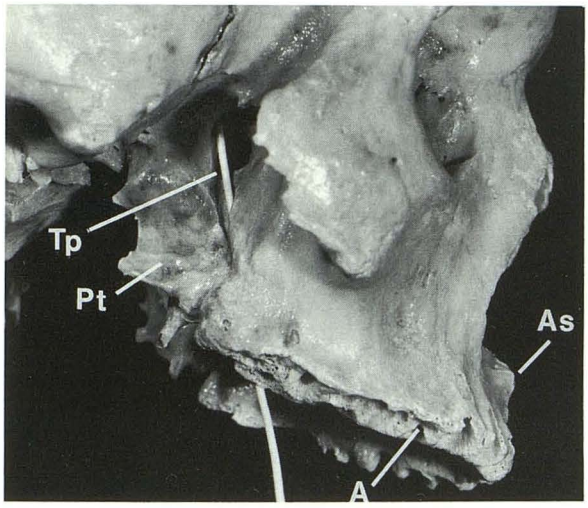

B

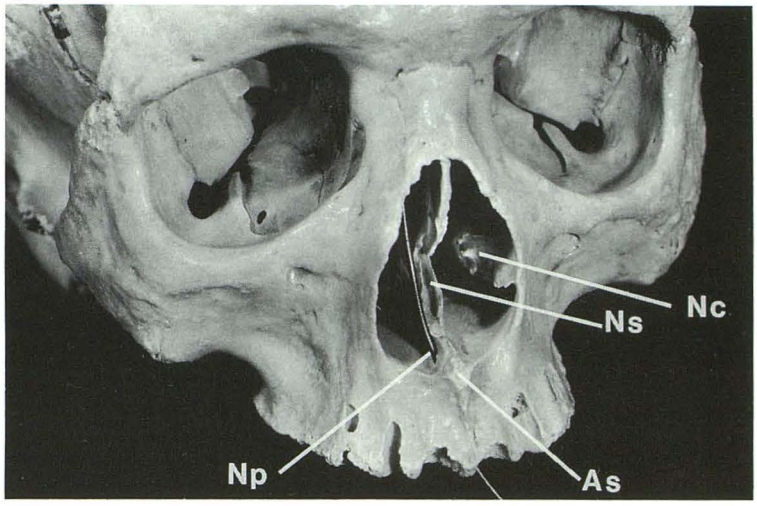

C

Fig. 7. Anatomic specimen demonstrating the inferior (*A*), lateral (*B*), and anterior (*C*) aspects of the maxilla. The white probe demonstrates the course of the greater palatine nerve; the black probe demonstrates the course of the nasopalatine nerve. *A* indicates alveolar process; *As*, anterior nasal spine; *G*, greater palatine foramen; *Gg*, groove for greater palatine nerve; *If*, incisive foramen; *L*, lesser palatine foramen; *Lt*, lateral pterygoid plate; *Mb*, maxillary bone: palatine process; *Mp*, median palatine suture; *Mt*, medial pterygoid; *Nc*, nasal conchi; *Np*, nasopalatine canal; *Ns*, nasal septum; *Pb*, palatine bone: horizontal plate; *Pt*, pterygoid process; *Tp*, pterygopalatine fossa; and *Ts*, transverse suture.

7C). After traversing the hard palate they form a common midline opening, the incisive foramen (*If* in 7A).

Lateral view

A portion of the zygomatic arch has been removed to demonstrate the pterygopalatine fossa (*Tp* in Fig. 7B), which is situated between the pterygoid process (*Pt* in Fig. 7B) and the posterior wall of the maxillary sinus. The white probe in the pterygopalatine fossa demonstrates the course of the pterygopalatine nerve. Inferiorly, the nerve exits the greater and lesser palatine foramina as the greater and lesser palatine nerves (Fig. 7A). The alveolar process (*A* in Fig. 7A and B) and the anterior nasal spine (*As* in Fig. 7B and C) are also identified.

Frontal view

The black probe, representing the course of the nasopalatine nerve, is seen entering the nasopalatine canal (*Np* in Fig. 7C) on either side of the nasal septum (*Ns* in Fig. 7C). These two canals will enter a common opening, the incisive foramen, on the inferior surface of the hard palate

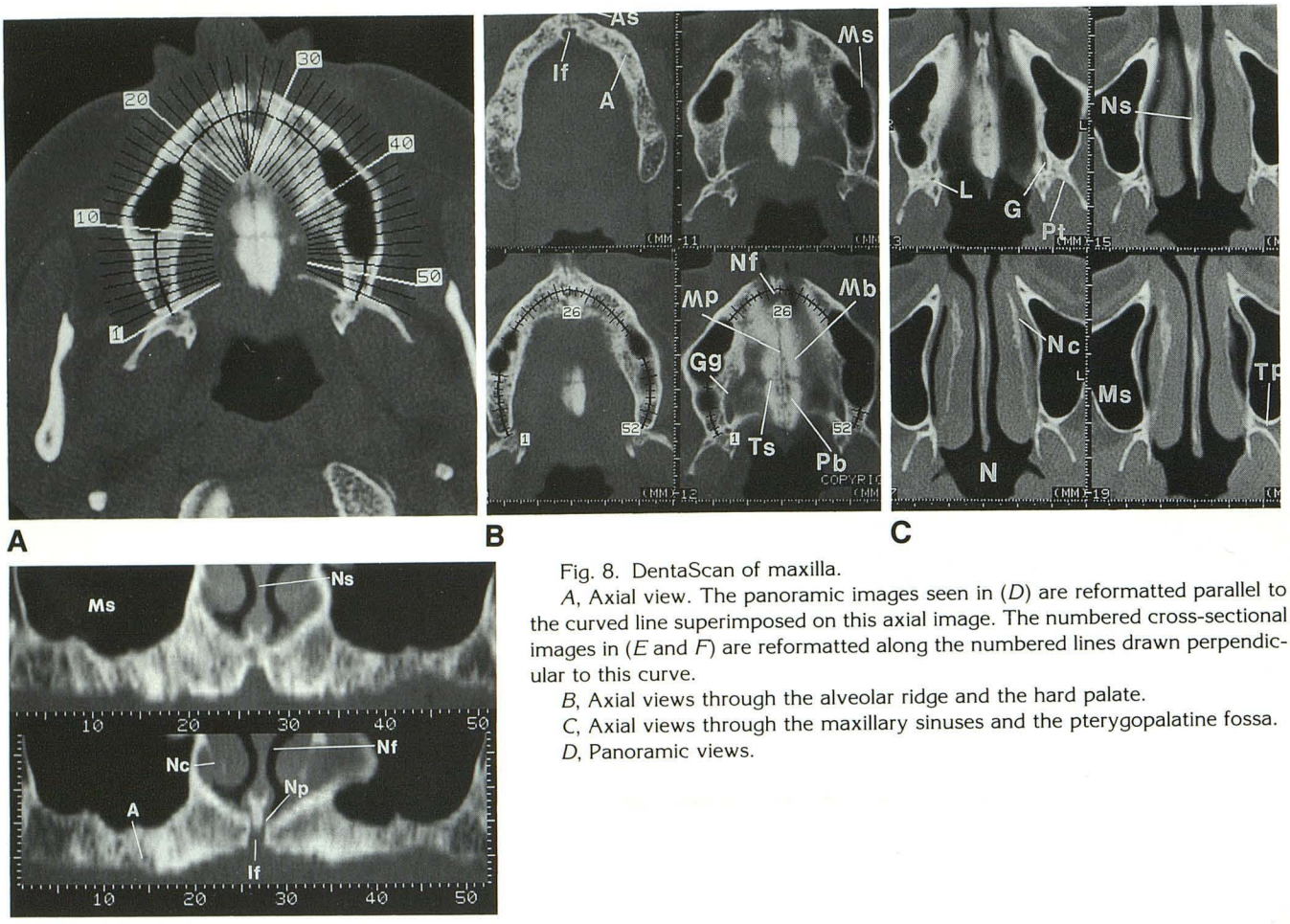

Fig. 8. DentaScan of maxilla.

A, Axial view. The panoramic images seen in (*D*) are reformatted parallel to the curved line superimposed on this axial image. The numbered cross-sectional images in (*E* and *F*) are reformatted along the numbered lines drawn perpendicular to this curve.

B, Axial views through the alveolar ridge and the hard palate.

C, Axial views through the maxillary sinuses and the pterygopalatine fossa.

D, Panoramic views.

(Fig. 7A). The nasal concha (*Nc* in Fig. 7C) and the anterior maxillary spine (*As* in Fig. 7C) are also seen.

DentaScan Images

Axial views

The more inferior axial images (Fig. 8B) demonstrate the incisive foramen (*If*) and the alveolar ridge (*A*). Teeth that are normally visualized in the alveolar process are absent in this edentulous maxilla. As one moves superiorly, the maxillary sinuses can be seen cephalad to the posterior aspect of the alveolar ridge; the nasal fossae (*Nf*) are seen cephalad to the anterior aspect of it. The right and left nasopalatine canals (Fig. 9A) appear as two separate openings until they merge to form a common opening, the incisive foramen (Fig. 9B), on the inferior aspect of the hard palate. At the level of the hard palate (Fig. 8B), the transverse suture (*Ts*) is visualized separating the maxillary bone (*Mb*) from the palatine bone (*Pb*). The right and left halves of these bones are defined by the median palatine suture (*Mp*). In the posterior hard palate just anterior to the pterygoid process (*Pt*), the greater (*G*) and lesser (*L*) palatine foramina are seen. The proximal portion of the groove (*Gg*) for the greater palatine nerve, which runs anteriomedially, is also visualized. On the more superior cuts (Fig. 8C), the nasal concha (*Nc*) and the nasal septum (*Ns*) are seen. The pterygopalatine fossa (*Tp*) is identified between the posterior wall of the maxillary sinus and the pterygoid process.

Panoramic view

Note how the maxillary sinuses (*Ms*) and the nasal fossae (*Nf*) are situated just cephalad to the alveolar process (*A*). The right and left nasopalatine canals (*Np*) are seen in the anterior inferior nasal fossa on either side of the nasal septum (*Ns*). The two canals merge to form a common opening, the incisive foramen (*If*).

Cross-sectional views

Images 1 through 27, represented here, correspond to the right half of the maxilla (see perpendicular lines 1 through 27 in Fig. 8A). Image 2, which is through the right posterior maxilla, demonstrates the greater palatine foramen (*G*) in cross-section. The proximal portion of the groove (*Gg*) for the greater palatine nerve is visualized in images 3 through 5. Note how the more posterior images (images 1 through 20) demonstrate the maxillary sinus (*Ms*) just cephalad to the alveolar ridge (*A*), whereas the more anterior images (images 21 through 30) demonstrate the nasal fossae (*Nf*) cephalad to it. In the midline (images 26

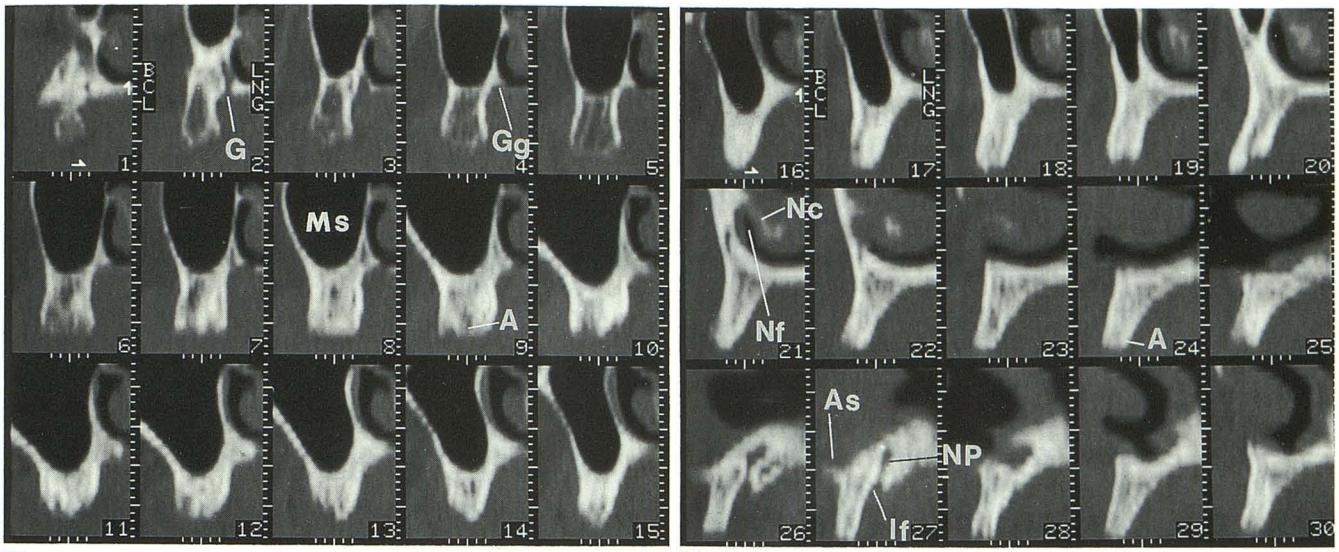

E F

Fig. 8. Continued.

E and *F*, Cross-sectional views. Images 1 through 15 (*E*) are through the posterior right maxilla (see perpendicular lines 1 through 15 in *A*); images 16 through 30 (*F*) are more anterior on the right and extend to the midline. The buccal (*BCL*) and lingual (*LNG*) surfaces are labeled in images 2 and 7. *A* indicates alveolar process; *As*, anterior nasal spine; *G*, greater palatine foramen; *Gg*, groove for greater palatine nerve; *If*, incisive foramen; *L*, lesser palatine foramen; *Lt*, lateral pterygoid plate; *Mb*, maxillary bone: palatine process; *Mp*, median palatine suture; *Ms*, maxillary sinus; *Mt*, medial pterygoid; *N*, nasopharynx; *Nc*, nasal conchi; *Nf*, nasal fossa; *Np*, nasopalatine canal; *Ns*, nasal septum; *Pb*, palatine bone: horizontal plate; *Pt*, pterygoid process; *Tp*, pterygopalatine fossa; *Ts*, transverse suture; and *Tg*, tongue.

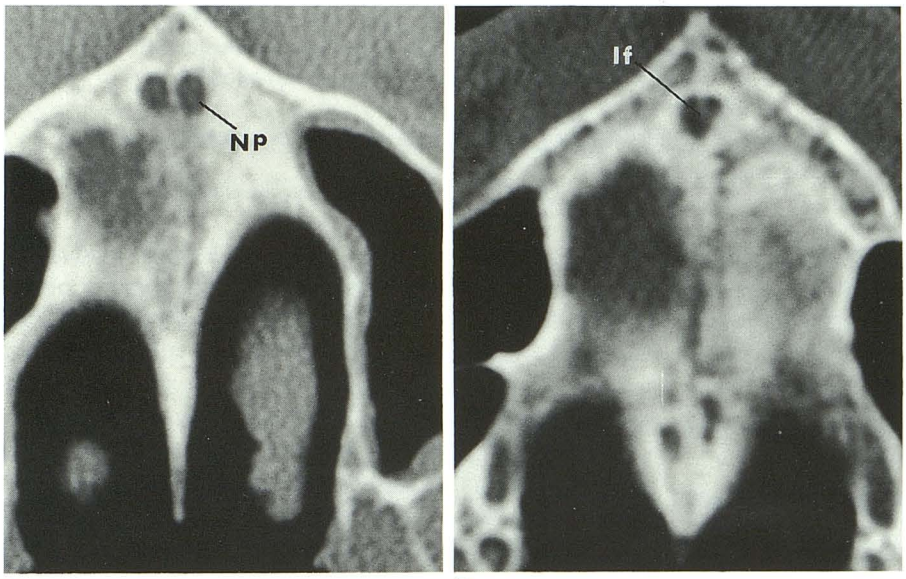

A B

Fig. 9. Axial view of the nasopalatine canal and the incisive foramen. The more superior axial image (*A*) demonstrates the two nasopalatine canals (*Np*); the inferior slice (*B*) demonstrates their common opening, the incisive foramen (*If*).

and 27), the nasopalatine canal (*Np*) and the incisive foramen (*If*) can be seen in cross-section. The anterior maxillary spine (*As*) is also seen in the midline. Note how the height, width, and contour of the alveolar ridge are clearly appreciated on the cross-sectional images.

Discussion

Dental reformatting programs provide excellent delineation of mandibular and maxillary anatomy. They are now being used to evaluate mandibular invasion by carcinoma of the oral cavity (6), degenerative changes of the temporomandibular joint (7), odontogenic cysts (5), fractures (8), oroantral fistulas (9), and position of foreign bodies (8). It should be pointed out that these images are designed for evaluating the osseous mandible and not the soft tissues. They are acquired by the use of a low-exposure technique, a bone

algorithm, and a dynamic mode. Magnetic resonance is excellent for evaluating the extraosseous soft tissue and may be necessary to use in conjunction with DentaScan. Patient motion artifact potentially can degrade these reformatted images, but I have not found this to be a problem.

References

1. Albrektsson T, Lekholm U. Osseointegration: current state of the art. *Dent Clin North Am* 1989;33:537–544
2. Schwarz MS, Rothman SLG, Rhodes ML, Chafetz N. Computer tomography: part I. Preoperative assessment of the mandible for endosseous implant surgery. *Int J Oral Maxillofac Implants* 1989;2:137–141
3. Schwarz MS, Rothman SLD, Rhodes ML, Chafetz N. Computer tomography: part II. Preoperative assessment of the maxilla for endosseous implant surgery. *Int J Oral Maxillofac Implants* 1987;2:143–148
4. Rothman SLG, Chafetz N, Rhodes ML, Schwartz MS. CT in the preoperative assessment of the mandible and maxilla for endosseous implant surgery. *Radiology* 1988;168:171–175
5. Abrahams JJ, Oliverio PJ. Odontogenic cysts: improved imaging with a dental CT software program. *AJNR: Am J Neuroradiol* 1993;14:367–374
6. Abrahams JJ, Friedman CD, Sasaki CT. Evaluation of neoplastic invasion of the mandible using DentaScan—a preliminary report. Presented at the 23rd Annual Meeting of the ASHNR, New Orleans, LA, 1990
7. Rabin DN, Rabin H, Sakowicz BA, Rabin MH, Rabin SI, Schwartz A. New techniques in dental surgical CT [abstract]. *Radiology* 1991;181(P):319
8. Abrahams JJ, Levine BP. Expanded applications of DentaScan (multiplanar computerized tomography of the mandible and maxilla). *Int J Periodont Rest Dent* 1990;10:465–472
9. Yanagisowa K, Friedman CT, Abrahams JJ, Vining E. DentaScan imaging of the mandible and maxilla. *Head Neck J* 1992 (in press)